Available online at www.sciencedirect.com
SCIENCE DIRECT®
Biochemical and Biophysical Research Communications 318 (2004) 227–233
BBRC
www.elsevier.com/locate/ybbrc

Characterization of recombinant soluble carcinoembryonic antigen cell adhesion molecule 1

Detlef Schumann,[a] Jie Huang,[b] Patrick E. Clarke,[c] Julia Kirshner,[b] Shih-wa Tsai,[a] Verne N. Schumaker,[d] and John E. Shively[a,*]

[a] *Division of Immunology, Beckman Research Institute of the City of Hope, Duarte, CA 91010, USA*
[b] *Graduate School of the City of Hope and Beckman Research Institute, Duarte, CA 91010, USA*
[c] *Division of Molecular Biology, Beckman Research Institute of the City of Hope, Duarte, CA 91010, USA*
[d] *Department of Chemistry and Biochemistry, Molecular Biology Institute, University of California at Los Angeles, Los Angeles, CA 90095, USA*

Received 1 April 2004

Abstract

Carcinoembryonic antigen cell adhesion molecule 1 (CEACAM1) is a type 1 transmembrane, homotypic cell adhesion protein expressed on epithelial and hematopoietic cells. CEACAM1 has four major isoforms with three or four immunoglobulin (Ig)-like ectodomains and either long or short cytoplasmic domains. In a 3D model of breast epithelial cell morphogenesis, CEACAM1 plays an essential role in lumen formation [J. Cell Sci. 112 (1999) 4193]. Two soluble ectodomain isoforms of CEACAM1 expressed in myeloma cells were immunologically active and highly glycosylated. The molecular weights of the 3-ecto- and 4-ectodomain isoforms were 90 and 110 kDa, respectively, and monomers by sedimentation equilibrium centrifugation. Both isoforms were prolate ellipsoids with axial ratios of 6 for the 3-ecto- and 8 for 4-ectodomain isoforms, respectively, by size exclusion chromatography and analytical ultracentrifugation. Both isoforms caused a significant reduction in lumen formation when tested in the 3D model culture system.

Keywords: CECAM1; Cell morphogenesis; Immunoglobulin domains; Sedimentation equilibrium; Analytical ultracentrifugation

Carcinoembryonic cell adhesion molecule 1 (CEACAM1, BGP, CD66a) is a type 1 transmembrane glycoprotein belonging to the carcinoembryonic antigen (CEA) gene family, which in turn is a member of the immunoglobulin (Ig) gene superfamily [1]. CEACAM1 is a 120–140 kDa glycoprotein with over 50% N-linked glycosylation by weight. It is expressed on the surface of a variety of epithelial and hematopoietic cells in human, rat, and mouse [2]. Human CEACAM1 has four major isoforms produced by alternative mRNA splicing, including three or four Ig-like ectodomains, and long (72 amino acids) or short (14 amino acids) cytoplasmic domains [3,4].

Murine CEACAM is a homotypic cell adhesion molecule [5] and a receptor for murine hepatitis virus [6], while human CEACAM1 is a receptor for *Neisseria gonorrhoeae* [7]. CEACAM1 expression is reduced in many cancers. For example, human CEACAM1 expression is downregulated in colon [8] and prostate carcinoma [9], and in 30% of breast tumors [10]. A potential role for CEACAM1 as a tumor inhibitor was shown by reversion of human prostate cancer tumors by transfection with the rat CEACAM1 gene [11] and reversion of the human mammary carcinoma cell phenotype in 3D culture by transfection with the human CEACAM1 gene [12].

CEACAM1 depends on the ecto N-domain for its cell–cell adhesion function [13] and phosphorylation of the long [14–16] and short [17] cytoplasmic domains for signal transduction. In addition, a key serine residue in murine CEACAM1 has been identified as a regulator for insulin clearance in liver in a transgenic mouse model [18,19]. Recently, we have demonstrated that CEACAM1 plays an essential role in lumen formation for the

* Corresponding author. Fax: 1-626-301-8186.
E-mail address: jshively@coh.org (J.E. Shively).

0006-291X/$ - see front matter © 2004 Elsevier Inc. All rights reserved.
doi:10.1016/j.bbrc.2004.04.024

breast epithelial cell line MCF10F grown in a 3D culture [20], while transfection of CECAM1 into the CEACAM1 negative breast tumor cell line MCF7 restored lumen formation [12], suggesting a role for CEACAM1 expression in mammary morphogenesis.

Until recently, little effort has been made to relate the structural properties of CEACAM1 to its various functions. The main obstacle to such studies has been the inability to express large amounts of the highly glycosylated glycoprotein in tissue culture and the fact that it is a type I transmembrane protein. In the case of CEA which is a GPI-linked glycoprotein and can be obtained in a soluble form, electron microscopy studies have described CEA as a rod shaped macromolecule with dimensions of $9\,\text{nm} \times 40\,\text{nm}$ [21]. A three-dimensional structure for CEA was predicted based on multiple sequence alignment with Ig fold structures [22] followed by an X-ray and neutron solution scattering study revealing an elongated molecule with a zig-zag arrangement of the Ig domains [23]. CEA in solution had a length of 27–33 nm and an X-ray radius of gyration R_G of 8 nm, consistent with an extended arrangement of seven domains. In contrast, the structure of CEACAM1 has been little studied, but it has been predicted to exist as either *cis* or *trans* dimers on the cell surface. A recombinant soluble isoform of murine CEACAM1a consisting of the extracellular domains 1 and 4 has been characterized by X-ray crystallography [24]. However, little is known about the biophysical characteristics of CEACAM1 and how these characteristics might be related to its functions. To characterize the properties of the more natural four and three extracellular domain isoforms of human CEACAM1, we expressed both human CEACAM1 isoforms as soluble recombinant proteins in NSO myeloma cells. Analytical ultracentrifugation of the affinity-purified proteins revealed that both isoforms exist as monomers in solution with a molecular weight of 90 kDa for the three domain isoform and 110 kDa for the four domain isoform. Both determined masses are in good agreement with the expected molecular weights for the post-translationally glycosylated isoforms of the proteins. Size exclusion chromatography and analytical ultracentrifugation further revealed that both soluble CEACAM1 isoforms are expressed as prolate ellipsoids with an axial ratio of 6 for the 3 domain isoform and 8 for the 4 domain isoform. Finally, both soluble isoforms showed biological activity in our 3D culture system of mammary morphogenesis. The availability of these recombinant constructs should facilitate studying the role of the two major ectodomain isoforms in the function of CEACAM1. The novel aspects of this study are directed at the problem of expressing and purifying highly glycosyated glycoproteins and the problem of characterization of them by conventional biophysical approaches.

Materials and methods

Construction of recombinant soluble CEACAM1. The extracellular domains of the full-length four domain CEACAM1–4L cDNA [25] were amplified using the forward primer BSRVN (5′-TTGATATC GTGACAGAGCAGCCGTGCTCGA-3′) and the reverse primer BSRVC (5′-TTGATATCTTACCCGGGTGAGAGGCCATTTTCT TG-3′). The primers introduced a stop codon after amino acid 364 (Gly) and added *Eco*RV sites to both the 5′ and 3′ untranslated regions of the resulting recombinant gene fragment. Additionally, the reverse primer introduced two silent mutations converting the Pro (363) Gly (364) sequence (CCGGGA) to a *Sma*I site (CCCGGG). The fragment was ligated into *Eco*RV restricted pBluescript vector (Stratagene) and the correct DNA sequence was verified. The recombinant CEACAM1–4 cDNA was ligated into *Sma*I restricted pEE12 expression vector [26]. The resulting plasmid pL202.9 was used for expression of soluble four domain CEACAM1 (CEACAM1–4sol). Soluble three domain CEACAM1 (CEACAM1–3sol) was constructed using the QuikChange Site-Directed Mutagenesis Kit (Stratagene) using the pL202.9 plasmid as a template. The forward BGPAB primer (5′-ACAGTCAAGAC GATCATAGTCACTCATCACCATCACCATCACTAACTAAGTC CAGTAGTAGCAAAG-3′) and the reverse -GPAB primer (5′-CTT TGCTACTACTGGACTTAGTTAGTGATGGTGATGGTGATGA GTGACTATGATCGTCTTGACTGT-3′) were designed to introduce a His_6-tag and a following stop codon after amino acid 255 (Thr). Introduction of the mutation was verified by DNA sequencing, and the resulting plasmid pBSAB5 was used for CEACAM1–3sol expression.

Transfection and expression of soluble CEACAM1. The expression vectors pL202.9 (CEACAM1–4sol) and pBSAB5 (CEACAM1–3sol) were transfected into NSO myeloma cells by electroporation. Transfected cells were incubated for 3 days at 37 °C in DMEM high glucose media (JRH Biosciences) containing 10% (v/v) FCS, 2 mM L-glutamine, and antibiotics. Viable cells were grown in 96-well microtiter plates at 5×10^3 cells/ml in L-glutamine deficient DMEM high glucose media containing 10% (v/v) dialyzed FCS, 2% (v/v) GS supplements (JRH Biosciences), and antibiotics. Expanded colonies were assayed for expression of the transfected protein and individual clones were isolated by serial dilution in 96-well microtiter plates.

Protein purification. Supernatants of confluent CEACAM1–4sol and CEACAM1–3sol cultures were collected, centrifuged at 3000 rpm for 15 min to remove cell debris, and stored at 4 °C. Stored supernatants were pooled prior to purification, adjusted to pH 7.5 using 1 M NaOH, and subjected to two filtration steps using 0.4 and 0.2 μm cellulose acetate filters. For CEACAM1–4sol, 500 ml of filtrate were passed over an affinity column using the murine CD66 specific monoclonal antibody T84.1 [27] immobilized on Poros EP epoxide resin (Applied Biosystems) on a BioCad Sprint liquid chromatography system (Applied Biosystems) at a flow rate of 0.5 ml/min and monitored at 280 nm. The column was washed with PBS until a stable baseline was reached, and the captured protein was eluted with 12 mM HCl/0.15 M NaCl. The eluate was adjusted to pH 7 using 1 M Tris base. For CEACAM1–3sol, 500 ml of filtrate was loaded at a flow rate of 0.5 ml/min on a Ni–NTA affinity column and monitored at 280 nm. Following the loading step the column was washed with PBS until a stable baseline was reached, and the captured protein was eluted using an imidazole gradient (0–0.1 M imidazole in 0.15 M NaCl/pH 7.4). Purified CEACAM1–4sol and CEACAM1–3sol were dialyzed against dH_2O at 4 °C, lyophilized, and stored at 4 °C.

Gel electrophoresis and Western blot analysis. Purified CEACAM1–4sol and CEACAM1–3sol (3.2 μg each) were analyzed by one-dimensional SDS-polyacrylamide (SDS–PAGE) or native gel electrophoresis on precast 8–16% Tris–glycine gradient gels (Invitrogen). For SDS–PAGE the proteins were mixed with 6× SDS sample buffer containing 0.35 M Tris–HCl, pH 6.8, 30% (v/v) glycerol, 10% (w/v) SDS, 0.6 M DTT, and 0.01% (w/v) bromophenol blue, heated to 95 °C for 5 min, and gel separated as previously described [28]. For native gel

electrophoresis the purified proteins were mixed with 6× non-denaturing sample buffer containing 0.35 M Tris–HCl, pH 6.8, 30% (v/v) glycerol, and 0.01% (w/v) bromophenol blue, and directly loaded on the gel. The native gel electrophoresis was performed in Tris base (24 mM) and glycine (192 mM) buffer. Gel separated proteins were either silver stained or transferred onto PVDF membranes (BioRad) using a semidry blotting system (BioRad). Blotted membranes were probed with mAb T84.1.

Size exclusion chromatography. Purified CEACAM1–4sol and CEACAM1–3sol were run individually (7.2 μg each) on a Superdex 200 HR10/30 size exclusion chromatography column (AP Biotech) and eluted with PBS (pH 7.4) at a flow rate of 0.5 ml/min on an Äkta Explorer 10 liquid chromatography system (AP Biotech). Elution was monitored at 280 nm. Molecular weight and molecular sizes were determined using a commercial SEC standard (BioRad) or a mixture of proteins with known Stokes radii.

Sedimentation velocity analysis. Velocity sedimentation was performed in a Beckman XL-A analytical ultracentrifuge (Beckman) in 0.0375 M NaCl, 0.025 M sodium phosphate, pH 7.0, and at 20 °C. Recombinant CEACAM1–4sol was analyzed at 52,000 rpm at a protein concentration of 0.36 mg/mL. Scans were taken at 8 min intervals. The scans were analyzed at a wavelength of 280 nm. Partial specific volume (υ) was calculated by assuming that the carbohydrate content was 50% high mannose (7 mannose and 2 *N*-acetylglucosamine residues per unit) and 50% complex (5 *N*-acetylglucosamine, 3 mannose, 3 galactose, 3 silaic acid, and 1 fucose residues per unit). The calculated υ for the carbohydrate was 0.625 mL/g and υ for the protein was assumed to be 0.725 mL/g. The average value used in the calculations was 0.675 mL/g, assuming 50% carbohydrates by weight. Recombinant CEACAM1–3sol was analyzed at 53,000 rpm at a protein concentration of 0.5 mg/mL, and scans were taken at 12 min intervals. A partial specific volume (υ) of 0.690 mL/g was calculated based on carbohydrate content and amino acid sequence. Sedimentation coefficients were calculated from measurements of the center of the symmetrical boundaries as a function of time and were corrected to the viscosity ($\eta/\eta_0 = 1.0174$) and density ($d = 1.0029$ g/mL) of water to obtain $s_{20,w}$. All sedimentation coefficients are reported as $s_{20,w}$ in Svedbergs (10^{-13} s).

Sedimentation equilibrium analysis. Sedimentation equilibrium experiments were performed in a Beckman XL-A analytical ultracentrifuge (Beckman), in 0.0375 M NaCl, 0.025 M sodium phosphate, pH 7.0, and at 20 °C. Recombinant CEACAM1–4sol was analyzed at 8500 rpm at a protein concentration of 0.36 mg/mL for 36 h. Recombinant CEACAM1–3sol was analyzed at 12,000 rpm at a protein concentration of 0.32 mg/mL for 40 h. The scans were analyzed at a wavelength of 280 and 235 nm, respectively, and at 20 °C. A wavelength of 235 nm was employed for some of the experiments due to limited quantities of protein.

Calculation of frictional coefficients and axial ratios. Frictional coefficients and axial ratios for both recombinant soluble CEACAM1 isoforms were calculated using the data derived from the sedimentation velocity and sedimentation equilibrium experiments using the formula:

$$s = \frac{M^{2/3}(1-\upsilon\rho)}{N6\pi\eta(1+(w/\upsilon\rho))^{1/3}(3\upsilon/4\pi N)^{1/3}(f/f_0)},$$

where s is the sedimentation coefficient ($\times 10^{13}$) determined from sedimentation velocity analysis, M is the molecular mass determined from sedimentation equilibrium analysis, N is Avogadro's number (6.02×10^{23}), υ is the partial specific volume of the molecule, ρ is the density of the solvent ($d = 1.0029$ g/mL), η is the viscosity of the solvent ($\eta/\eta_0 = 1.0174$), and $w = 0.7$ (hydration in g water/g protein).

Three-dimensional culture. Cells (2.5×10^5) were plated in a thick layer (1 mm) of Matrigel (BD) in the 2-well chamber slides (Nunc). Solidified Matrigel was overlaid with 2 ml/well of mammary epithelial cell growth medium (MEGM) supplemented with SingleQuots (Clonetics). Cells were grown in Matrigel as described previously [12]. All treatments were added to the media and changed every other day. Cells grown in Matrigel were scored for the presence or absence of lumens. Statistical analysis was done by the χ^2 test.

Results and discussion

Expression and purification of soluble CEACAM1

Recombinant CEACAM1–3sol and CEACAM1–4sol were expressed as secreted proteins in NSO myeloma cells and purified by one-step chromatography from the supernatants of selected clones. The presence of a His_6-tag allowed the purification of CEACAM1–3sol by Ni–NTA chromatography, while CEACAM1–4sol was purified on an antibody-affinity column using the immobilized CD66 specific mAb T84.1. The purity of both recombinant soluble CEACAM1 isoforms was assessed by SDS–PAGE and Western blot analysis (Fig. 1). CEACAM1–3sol gave a major diffuse band with an estimated molecular weight of 90 kDa, in line with the expected molecular weight of three glycosylated Ig-like extracellular domains with nine N-glycosylation sites. Similarly, CEACAM1–4sol had an estimated molecular weight of 110 kDa, as expected for four glycosylated Ig-like extracellular domains.

CEACAM1–3sol and CEACAM1–4sol are monomers in solution

Previous studies have shown that CEACAM1 acts as a homotypic cell–cell adhesion molecule with predicted *cis* and *trans* homodimer formation at the cell surface [2]. To investigate whether CEACAM1–3sol and CEACAM1–4sol exhibited formation of non-covalent dimers, both soluble CEACAM1 isoforms were analyzed by size exclusion chromatography (SEC) on a Superdex

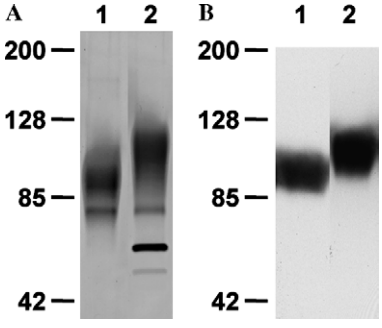

Fig. 1. SDS–PAGE and Western blot analysis of soluble CEACAM1 isoforms. Purified CEACAM1–3sol (lane 1) and CEACAM1–4sol (lane 2) were run on 8–16% gradient Tris–glycine gels (Invitrogen) and silver stained or transferred to PVDF membrane for subsequent immunoblotting. (A) Soluble CEACAM1 isoforms were run under reducing conditions on an SDS gel. (B) Western blot analysis of purified soluble CEACAM1 isoforms. *Note.* the additional band at 50 kDa for CEACAM1–4sol is due to trace amounts of co-eluted T84.1 heavy chain from the affinity column.

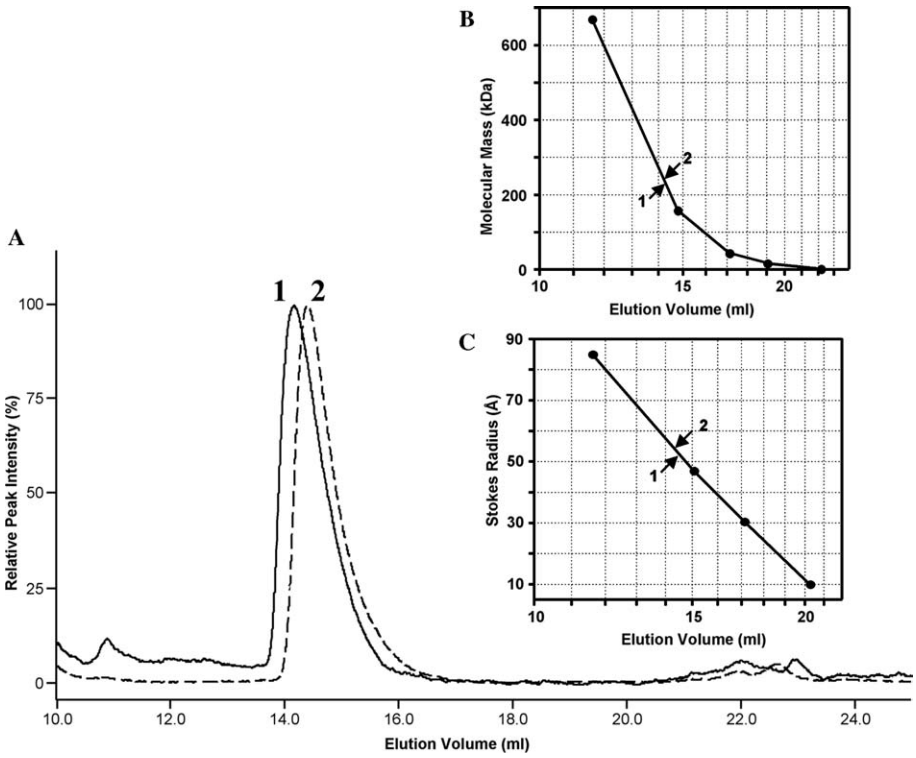

Fig. 2. Size exclusion chromatography of soluble CEACAM1 isoforms. Purified CEACAM1sol1 and CEACAM1sol2 were run individually (7.2 μg each) on a Superdex 200 HR10/30 column (Amersham–Pharmacia) and eluted with PBS (pH 7.4) at a flow rate of 0.5 ml/min. Protein elution was monitored at 280 nm. (A) Superimposed elution profiles of CEACAM1–3sol (1; dashed line) and CEACAM1–4sol (2; solid line). (B) Determination of the molecular weight of CEACAM1–3sol (1; 210 kDa) and CEACAM1–4sol (2; 240 kDa) using the BioRad SEC calibration standard. (C) Determination of the Stokes radii of CEACAM1–3sol (1; 53 Å) and CEACAM1–4sol (2; 56 Å) using a mixture of proteins with known Stokes radii as a calibration standard.

200 HR10/30 column. Both isoforms exhibited a single peak (Fig. 2A) with apparent molecular weights of 210 and 240 kDa for CEACAM1–3sol and CEACAM1–4sol, respectively. In both cases the molecular weights determined by SEC were about twofold higher than those determined by SDS–PAGE. The difference in these findings could be explained either by nearly complete dimer formation of soluble CEACAM1 molecules, which would be separated into monomers under the denaturing conditions of SDS–PAGE, or by a non-globular shape during SEC elution. Since SEC separates proteins according to their molecular size and shape rather than their molecular weight (Fig. 2B), we first established the Stokes radius of the two soluble isoforms using calibrants of known Stokes radii (Fig. 2C). Compared to bovine serum albumin, a globular 66 kDa protein with a Stokes radius of 35.5 Å, or yeast alcohol dehydrogenase, a globular 150 kDa protein with a Stokes radius of 46 Å, the Stokes radii calculated for CEACAM1–3sol and –4sol were 53 and 56 Å, respectively, indicating that both soluble isoforms were elongated rather than globular proteins. When both isoforms were subjected to sedimentation equilibrium experiments in an analytical ultracentrifuge (Figs. 3A and B), molecular weights of 90,000 and 110,000 Da were obtained for the –3sol and –4sol isoforms, respectively, confirming the results of the SDS–PAGE analysis.

CEACAM1–3sol and CEACAM1–4sol are prolate ellipsoids in solution

To obtain more conclusive information about the shape of these molecules, we performed sedimentation velocity experiments on both soluble CEACAM1 isoforms. The sedimentation coefficients obtained from these experiments in combination with the results of the previous sedimentation equilibrium experiments allow a calculation of the frictional coefficients and the axial ratios, which are measures of the molecular asymmetry of the analyzed molecules. A corrected s value of 5.17 was obtained for CEACAM1–3sol (Fig. 3D), with a frictional ratio, f/f_0 of 1.32. This compares to 1.14 for ribonuclease, a globular protein, and 2.38 for fibrinogen, a prolate ellipsoid. Using a table derived by Cantor and Schimmel [29], which illustrates the relation of the frictional ratio of a protein to its axial ratio a/b, where a and b are the major and minor axes of the prolate ellipsoid, respectively, we conclude that CEACAM1–3sol is a prolate ellipsoid with an axial ratio of 6. Similarly,

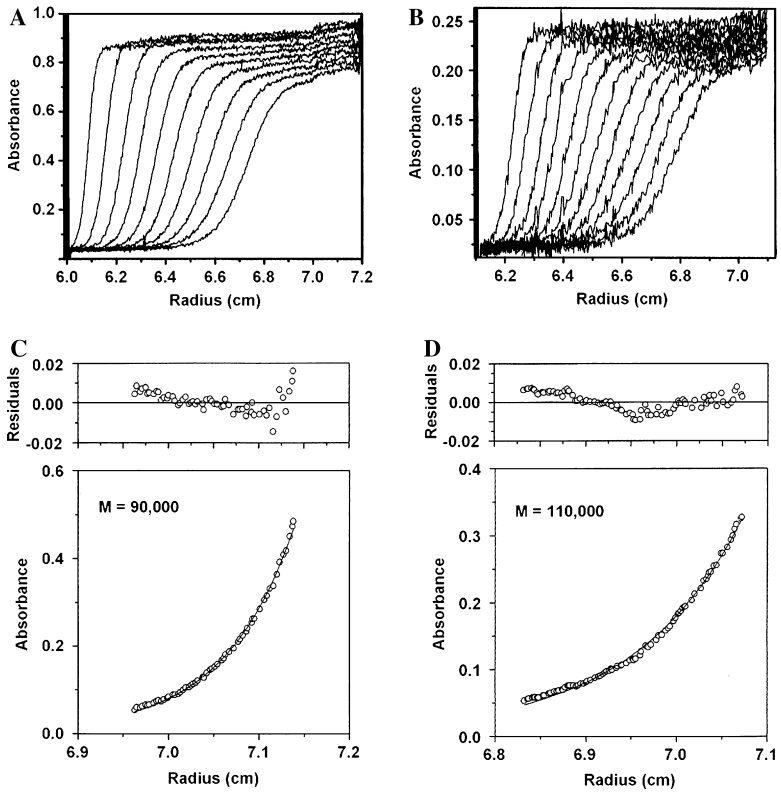

Fig. 3. Sedimentation velocity and equilibrium analysis of soluble CEACAM1 isoforms. Sedimentation velocity and equilibrium experiments were performed in a Beckman XL-A ultracentrifuge. Sedimentation coefficients were calculated from the sedimentation profiles by measuring the centers of the symmetrical boundaries. (A) Analysis of CEACAM1–3sol (0.5 mg/ml) was performed at 53,000 rpm and 20 °C at 12 min intervals. (B) Analysis of CEACAM1–4sol (0.36 mg/ml) was performed at 52,000 rpm and 20 °C at 8 min intervals. For sedimentation equilibrium experiments, lower panels show data plotted as absorbance (280 nm) vs. radial distance (cm) and upper panels show plots of best-fit residuals vs. radial distance. (C) Analysis of CEACAM1–3sol (0.32 mg/ml) was performed at 12,000 rpm and 20 °C for 40 h. Using a boundary best fit with a single exponential a molecular weight of 90,000 Da was calculated. (D) Analysis of CEACAM1–4sol (0.36 mg/ml) was performed at 8500 rpm and 20 °C for 36 h. A molecular weight of 110,000 Da was calculated using a boundary best fit with a single exponential.

sedimentation velocity analysis of CEACAM1–4sol gives a corrected s value of 5.6 and a frictional ratio f/f_0 of 1.43 for CEACAM1–4sol (Fig. 3D). Using these data we calculate an axial ratio of 8 for CEACAM1–4sol. The results of the analytical ultracentrifugation experiments therefore indicate that while both isoforms exist as monomers in solution (at the concentrations used), their ellipsoid shape and their large axial ratio cause them to show elution characteristics in SEC that are similar to those of globular molecules twice their molecular weight. The elongated shape of these soluble isoforms of CEACAM1 agrees with the shape determined for human CEA [23] and the two domain structure of murine CEACAM1 [24].

The inability of homotypic cell adhesion molecules to form dimers in solution is not unusual. The classic example is soluble E-cadherin for which dimers were not obtained over a wide range of concentrations [30]. In order to demonstrate dimers in a crystal structure, it was necessary to make soluble E-cadherin fusion proteins with a dimerization domain [31] or disulfide-linked dimers [32]. On the other hand, *cis* dimers were obtained for N-CAM [33] and C-CAM [34], with implications for formation of *trans* dimers between two cells. It should be noted that the absence of dimers in solution does not rule out dimerization at the cell surface where unusually high concentrations of spatially constrained membrane oriented molecules are achieved. In order to compare CEACAM1 ectodomains to other cadherins, it may be necessary to also fuse them to a dimerization domain. Nonetheless, our data demonstrate that the soluble forms of CEACAM1 are elongated monomers in solution, similar to the structure of other cadherins.

CEACAM1–3sol and CEACAM1–4sol inhibit lumen formation in a 3D culture model

To test the recombinant soluble CEACAM1 isoforms in a biologically relevant assay, both ioforms were added to cultures of CEACAM1–4S transfected MCF-7 cells in a 3D Matrigel assay system (Table 1). Compared to the untreated control, continued incubation of the cells with the soluble isoforms for 12 days resulted in a reduction of lumen formation from 65.0% (control) to

Table 1
Effect of soluble CEACAM1 on acini formation

Cell	Treatment	Amount (μM)	% Lumen	*N*	*P* value
MCF7/CEACAM1–4S	None	—	65.0	226	
MCF7/CEACAM1–4S	3sol	0.4	49.5	189	<0.01
MCF7/CEACAM1–4S	4sol	0.4	40.7	131	<0.001

CEACAM1–4S transfected MCF7 cells (2.5×10^5 per well) were grown in Matrigel in the presence of indicated amounts of CEACAM1–3sol (3sol) or CEACAM1–4sol (4sol). After 12 days the cells were fixed, embedded in paraffin, stained with anti-CEACAM1 mAb 4D1C2, and scored for lumen formation. *N*, number of colonies scored. *P* values were calculated by χ^2 test compared to the non-treated control.

49.5% ($P < 0.01$), or 40.7% ($P < 0.001$) for CEACAM1–3sol or CEACAM1–4sol, respectively. Although limited quantities of both recombinant soluble CEACAM1 isoforms prevented us from performing dose–response studies, the reduction of lumen formation by CEACAM1–4sol is similar to our previously reported effect of soluble CEACAM1–4sol on lumen formation using the breast cell line MCF10F in the Matrigel assay [20]. Therefore, we now demonstrate that both soluble CEACAM1 isoforms have a similar effect on lumen formation in our test system, with the possible conclusion that the –3sol isoform is less effective than the –4sol isoform when inhibiting cells transfected with the –4S isoform. We can also conclude that both isoforms are sufficently folded and biologically active to cause a disruption of inter- and intracellular CEACAM1 interactions at the cell surface of MCF7/CEACAM1–4S cells, which ultimately leads to a decrease in their ability to form glandular structures in a basal membrane environment. Thus, monomer soluble isoforms are able to interact with membrane bound forms in whatever state of aggregation present.

Acknowledgment

This work was supported by NIH Grant CA84202.

References

[1] A.F. Williams, A.N. Barclay, The immunoglobulin superfamily-domains for cell surface recognition, Annu. Rev. Immunol. 6 (1988) 381.
[2] B. Obrink, CEA adhesion molecules: multifunctional proteins with signal-regulatory properties, Curr. Opin. Cell Biol. 9 (1997) 616.
[3] T. Barnett, S.J. Goebel, M.A. Nothdurft, J.J. Elting, Carcinoembryonic antigen family: characterization of cDNAs coding for NCA and CEA and suggestion of nonrandom sequence variation in their conserved loop-domains, Genomics 3 (1988) 59.
[4] T.R. Barnett, L. Drake, W. Pickle 2nd, Human biliary glycoprotein gene: characterization of a family of novel alternatively spliced RNAs and their expressed proteins, Mol. Cell. Biol. 13 (1993) 1273.
[5] C. Turbide, M. Rojas, C.P. Stanners, N. Beauchemin, A mouse carcinoembryonic antigen gene family member is a calcium-dependent cell adhesion molecule, J. Biol. Chem. 266 (1991) 309.
[6] G.S. Dveksler, C.W. Dieffenbach, C.B. Cardellichio, K. McCuaig, M.N. Pensiero, G.S. Jiang, N. Beauchemin, K.V. Holmes, Several members of the mouse carcinoembryonic antigen-related glycoprotein family are functional receptors for the coronavirus mouse hepatitis virus-A59, J. Virol. 67 (1993) 1.
[7] S.D. Gray-Owen, C. Dehio, A. Haude, F. Grunert, T.F. Meyer, CD66 carcinoembryonic antigens mediate interactions between Opa-expressing *Neisseria gonorrhoeae* and human polymorphonuclear phagocytes, Embo J. 16 (1997) 3435.
[8] M. Neumaier, S. Paululat, A. Chan, P. Matthaes, C. Wagener, Biliary glycoprotein, a potential human cell adhesion molecule, is down-regulated in colorectal carcinomas, Proc. Natl. Acad. Sci. USA 90 (1993) 10744.
[9] D.I. Kleinerman, P. Troncoso, S.H. Lin, L.L. Pisters, E.R. Sherwood, T. Brooks, A.C. von Eschenbach, J.T. Hsieh, Consistent expression of an epithelial cell adhesion molecule (C-CAM) during human prostate development and loss of expression in prostate cancer: implication as a tumor suppressor, Cancer Res. 55 (1995) 1215.
[10] J. Huang, J.F. Simpson, C. Glackin, L. Riethorf, C. Wagener, J.E. Shively, Expression of biliary glycoprotein (CD66a) in normal and malignant breast epithelial cells, Anticancer Res. 18 (1998) 3203.
[11] J.T. Hsieh, W. Luo, W. Song, Y. Wang, D.I. Kleinerman, N.T. Van, S.H. Lin, Tumor suppressive role of an androgen-regulated epithelial cell adhesion molecule (C-CAM) in prostate carcinoma cell revealed by sense and antisense approaches, Cancer Res. 55 (1995) 190.
[12] J. Kirshner, C.J. Chen, P. Liu, J. Huang, J.E. Shively, CEACAM1–4S, a cell–cell adhesion molecule, mediates apoptosis and reverts mammary carcinoma cells to a normal morphogenic phenotype in a 3D culture, Proc. Natl. Acad. Sci. USA 100 (2003) 521.
[13] S.M. Watt, A.M. Teixeira, G.Q. Zhou, R. Doyonnas, Y. Zhang, F. Grunert, R.S. Blumberg, M. Kuroki, K.M. Skubitz, P.A. Bates, Homophilic adhesion of human CEACAM1 involves N-terminal domain interactions: structural analysis of the binding site, Blood 98 (2001) 1469.
[14] D.E. Afar, C.P. Stanners, J.C. Bell, Tyrosine phosphorylation of biliary glycoprotein, a cell adhesion molecule related to carcinoembryonic antigen, Biochim. Biophys. Acta 1134 (1992) 46.
[15] K.M. Skubitz, T.P. Ducker, S.A. Goueli, CD66 monoclonal antibodies recognize a phosphotyrosine-containing protein bearing a carcinoembryonic antigen cross-reacting antigen on the surface of human neutrophils, J. Immunol. 148 (1992) 852.
[16] M. Huber, L. Izzi, P. Grondin, C. Houde, T. Kunath, A. Veillette, N. Beauchemin, The carboxyl-terminal region of biliary glycoprotein controls its tyrosine phosphorylation and association with protein-tyrosine phosphatases SHP-1 and SHP-2 in epithelial cells, J. Biol. Chem. 274 (1999) 335.
[17] M. Edlund, K. Wikstrom, R. Toomik, P. Ek, B. Obrink, Characterization of protein kinase C-mediated phosphorylation of the short cytoplasmic domain isoform of C-CAM, FEBS Lett. 425 (1998) 166.

[18] M.N. Poy, R.J. Ruch, M.A. Fernstrom, Y. Okabayashi, S.M. Najjar, Shc and CEACAM1 interact to regulate the mitogenic action of insulin, J. Biol. Chem. 277 (2002) 1076.
[19] M.N. Poy, Y. Yang, K. Rezaei, M.A. Fernstrom, A.D. Lee, Y. Kido, S.K. Erickson, S.M. Najjar, CEACAM1 regulates insulin clearance in liver, Nat. Genet. 30 (2002) 270.
[20] J. Huang, J.D. Hardy, Y. Sun, J.E. Shively, Essential role of biliary glycoprotein (CD66a) in morphogenesis of the human mammary epithelial cell line MCF10F, J. Cell Sci. 112 (1999) 4193.
[21] H.S. Slayter, J.E. Coligan, Electron microscopy and physical characterization of the carcinoembryonic antigen, Biochemistry 14 (1975) 2323.
[22] P.A. Bates, J. Luo, M.J. Sternberg, A predicted three-dimensional structure for the carcinoembryonic antigen (CEA), FEBS Lett. 301 (1992) 207.
[23] M.K. Boehm, A.L. Corper, T. Wan, M.K. Sohi, B.J. Sutton, J.D. Thornton, P.A. Keep, K.A. Chester, R.H. Begent, S.J. Perkins, Crystal structure of the anti-(carcinoembryonic antigen) single-chain Fv antibody MFE-23 and a model for antigen binding based on intermolecular contacts, Biochem. J. 346 (Pt. 2) (2000) 519.
[24] K. Tan, B.D. Zelus, R. Meijers, J.H. Liu, J.M. Bergelson, N. Duke, R. Zhang, A. Joachimiak, K.V. Holmes, J.H. Wang, Crystal structure of murine sCEACAM1a[1,4]: a coronavirus receptor in the CEA family, Embo J. 21 (2002) 2076.
[25] Y. Hinoda, M. Neumaier, S.A. Hefta, Z. Drzeniek, C. Wagener, L. Shively, L.J.F. Hefta, J.E. Shively, R.J. Paxton, Molecular cloning of a cDNA coding biliary glycoprotein I: primary structure of a glycoprotein immunologically crossreactive with carcinoembryonic antigen, Proc. Natl. Acad. Sci. USA 85 (1988) 6959.
[26] C.R. Bebbington, G. Renner, S. Thomson, D. King, D. Abrams, G.T. Yarranton, High-level expression of a recombinant antibody from myeloma cells using a glutamine synthetase gene as an amplifiable selectable marker, Biotechnology (NY) 10 (1992) 169.
[27] C. Wagener, B.R. Clark, K.J. Rickard, J.E. Shively, Monoclonal antibodies for carcinoembryonic antigen and related antigens as a model system: determination of affinities and specificities of monoclonal antibodies by using biotin-labeled antibodies and avidin as precipitating agent in a solution phase immunoassay, J. Immunol. 130 (1983) 2302.
[28] U.K. Laemmli, Cleavage of structural proteins during the assembly of the head of bacteriophage T4, Nature 227 (1970) 680.
[29] C.R. Cantor, P.R. Schimmel, Biophysical Chemistry Part II: Techniques for the Study of Biological Structure and Function, W.H. Freeman & Co, New York, 1980.
[30] M. Overduin, T.S. Harvey, S. Bagby, K.I. Tong, P. Yau, M. Takeichi, M. Ikura, Solution structure of the epithelial cadherin domain responsible for selective cell adhesion, Science 267 (1995) 386.
[31] O. Pertz, D. Bozic, A.W. Koch, C. Fauser, A. Brancaccio, J. Engel, A new crystal structure, Ca^{2+} dependence and mutational analysis reveal molecular details of E-cadherin homoassociation, Embo J. 18 (1999) 1738.
[32] I.T. Makagiansar, P.D. Nguyen, A. Ikesue, K. Kuczera, W. Dentler, J.L. Urbauer, N. Galeva, M. Alterman, T.J. Siahaan, Disulfide bond formation promotes the *cis*- and *trans*-dimerization of the E-cadherin-derived first repeat, J. Biol. Chem. 277 (2002) 16002.
[33] K. Tamura, W.S. Shan, W.A. Hendrickson, D.R. Colman, L. Shapiro, Structure–function analysis of cell adhesion by neural (N-) cadherin, Neuron 20 (1998) 1153.
[34] T.J. Boggon, J. Murray, S. Chappuis-Flament, E. Wong, B.M. Gumbiner, L. Shapiro, C-cadherin ectodomain structure and implications for cell adhesion mechanisms, Science 296 (2002) 1308.